THE JOURNAL OF PHYSICAL CHEMISTRY Letters

Letter

pubs.acs.org/JPCL

Large-Scale Density Functional Theory Transition State Searching in Enzymes

Greg Lever,*[,†] Daniel J. Cole,[†,‡] Richard Lonsdale,[¶] Kara E. Ranaghan,[¶] David J. Wales,[§] Adrian J. Mulholland,[¶] Chris-Kriton Skylaris,[∥] and Mike C. Payne[†]

[†]Theory of Condensed Matter Group, Cavendish Laboratory, 19 JJ Thomson Avenue, Cambridge CB3 0HE, United Kingdom

[‡]Department of Chemistry, Yale University, New Haven, Connecticut 06520-8107, United States

[¶]Centre for Computational Chemistry, School of Chemistry, University of Bristol, Bristol BS8 1TS, United Kingdom

[§]University Chemical Laboratory, Lensfield Road, Cambridge CB2 1EW, United Kingdom

[∥]School of Chemistry, University of Southampton, Highfield, Southampton SO17 1BJ, United Kingdom

Supporting Information

ABSTRACT: Linear-scaling quantum mechanical density functional theory calculations have been applied to study the rearrangement of chorismate to prephenate in large-scale models of the *Bacillus subtilis* chorismate mutase enzyme. By treating up to 2000 atoms at a consistent quantum mechanical level of theory, we obtain an unbiased, almost parameter-free description of the transition state geometry and energetics. The activation energy barrier is calculated to be lowered by 10.5 kcal mol^{-1} in the enzyme, compared with the equivalent reaction in water, which is in good agreement with experiment. Natural bond orbital analysis identifies a number of active site residues that are important for transition state stabilization in chorismate mutase. This benchmark study demonstrates that linear-scaling density functional theory techniques are capable of simulating entire enzymes at the ab initio quantum mechanical level of accuracy.

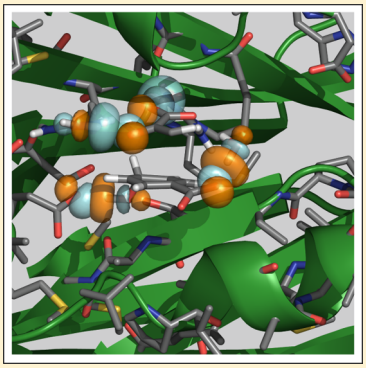

SECTION: Biophysical Chemistry and Biomolecules

Accurate computational prediction of activation energy barriers and mechanisms of rate enhancement in enzymes could contribute significantly to pharmaceutical inhibitor development and biomimetic catalyst design. In this context, combined quantum mechanical/molecular mechanical (QM/MM) simulations, in which the substrate is treated with a QM method and the surrounding enzyme and water molecules are treated with classical point charges, are an invaluable tool. Indeed, recent advances in the treatment of electron correlation provide a well-established methodological hierarchy, which has been shown to reproduce activation energy barriers to chemical accuracy (within 1 kcal mol^{-1}) as part of the QM/MM framework.[1] With these advances, the focus in computational enzymology now is on testing and improving the QM/MM methodology itself, rather than the level of QM theory.[1,2] It is clear that a MM treatment does not include electronic effects, such as charge transfer between the substrate and protein, and the QM/MM partitioning could potentially suffer from the so-called electron leakage effect, whereby point charges over-polarize the electron density.[3] The classical force field may also correspond to an incorrect description of the electrostatic environment[4] or intramolecular strain, or, in cases of covalent bonding between the QM and MM regions, the method may be sensitive to the link algorithm employed. It has been suggested that such effects may limit the accuracy of QM/MM modeling of enzyme-catalyzed reactions.[2] There is a clear need for methods capable not only of incorporating and analyzing electronic effects on the large scale in proteins[5] but also of optimizing transition state (TS) structures in this context. In this regard, promise is shown by large-scale density functional theory (DFT), which is capable of providing an accurate QM description of molecular systems comprising thousands of atoms,[6−8] thus making it particularly suited to the study of the function of biomolecular systems.[9−18] Comprehensive reviews of $O(N)$ DFT methods and their applications can be found elsewhere.[19,20] These techniques can be used to investigate the physical nature of interactions in proteins and enzyme catalysis and also provide a benchmark for hybrid or empirical methods. Here, we demonstrate that TS optimization is now possible in large-scale QM calculations on enzyme-catalyzed reactions. To show this, we employ the linear-scaling density functional theory (LS-DFT) code, ONETEP,[21] to perform fully quantum mechanical TS searching calculations in large-scale models (up to 2000 atoms) of the chorismate mutase (CM) enzyme and in water.

Received: September 3, 2014
Accepted: October 7, 2014
Published: October 7, 2014

   dx.doi.org/10.1021/jz5018703 | *J. Phys. Chem. Lett.* 2014, 5, 3614−3619

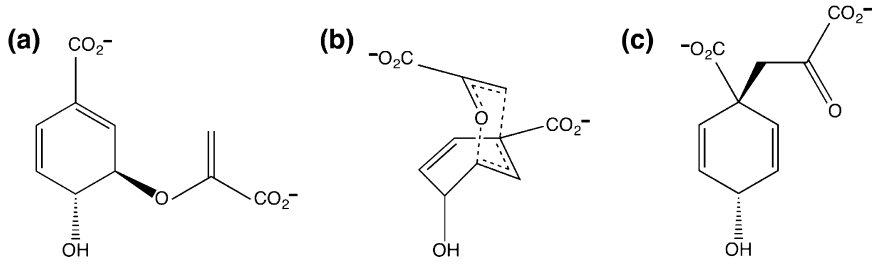

Figure 1. Rearrangement of (a) chorismate, via (b) the TS, to (c) prephenate.

Situated at a branch point in the shikimate pathway, which is crucial for generating aromatic amino acids, CM catalyzes the Claisen rearrangement of chorismate to prephenate (Figure 1). Due to (i) the lack of covalent bonding between the substrate and enzyme active site,[22] (ii) the fact that the reaction also occurs in water with a similar mechanism, and (iii) the availability of experimental data,[22−24] this has become a model system for benchmarking computational methodologies.[1,25,26] In the present work, we have performed LS-DFT structural optimizations of CM with the PBE exchange−correlation functional[27] to demonstrate the feasibility of performing large-scale TS searching in enzymes, with every atom treated at the QM level. Initial reactant state (RS) and product state (PS) structures, both in CM and in water, were generated via semiempirical QM/MM molecular dynamics, followed by B3LYP/MM optimization,[26] from which spherical clusters were extracted and reoptimized using the ONETEP LS-DFT code.[21,28] TS searching was initially performed according to a modified linear and quadratic synchronous transit (LST/QST) pathway approach,[29] in combination with conjugate gradient optimization. The LST/QST algorithm takes as input only the optimized coordinates of the beginning and end states and does not require any a priori knowledge of the TS structure, as is often the case in reaction-coordinate-based methods. Extensive convergence tests were performed to determine the reliability of the results. Refinement of the TS for the chorismate to prephenate rearrangement in vacuum generated by the LST/QST algorithm using the gradient-only version of hybrid eigenvector-following[30] reduced the activation energy barrier by less than 0.1 kcal mol^{-1} (Supporting Information (SI) section S2.3). This small change upon precise optimization probably reflects the relatively straightforward nature of the pathway in this case. Table 1 demonstrates convergence of the activation energy barrier and reaction energy with respect to the size of the system and the number of mobile and frozen atoms for clusters comprising up to 1999 atoms. The maximum change in energy is just 0.3 kcal mol^{-1}. Similar results were obtained for the reaction in water, although a larger mobile region was required (SI section S1.3).

Table 1. Energy Difference Convergence[a]

mobile	frozen	$\Delta^{\ddagger}E$	ΔE
98	901	13.4	−7.7
211	788	13.5	−8.0
98	1901	13.3	−7.9

[a]Convergence of the activation ($\Delta^{\ddagger}E$) and reaction (ΔE) energies (kcal mol^{-1}) in CM for a number of model systems with different numbers of mobile and frozen atoms. Mobile atoms are allowed to relax during optimization and TS searching, while frozen atoms are fixed to the B3LYP/MM geometry.

Our convergence tests indicate that for CM, a computational model comprising a ∼100 atom mobile region within a larger ∼1000 atom cluster, in vacuum, provides an accurate description of the energetics of this system. This model was therefore used to compute the energetics of the chorismate to prephenate rearrangement in CM, and the results were averaged over five different pathways to account for temperature-induced fluctuations.[26] Figure 2 shows exemplar geometries of the optimized RS and PS structures, as well as the TS generated from LS-DFT, all of which are in excellent agreement with B3LYP/MM geometries.[26] Table 2 shows the final averaged activation and reaction energies for the chorismate to prephenate rearrangement in both CM and water. The barrier height in the enzyme is in good agreement with experiment, while in water, both the activation and reaction energies are too positive by about 4 kcal mol^{-1}. The change in the activation barrier in CM is predicted to be −10.5 kcal mol^{-1}, while the reaction energy is similar in the two environments (difference of 1.6 kcal mol^{-1}). The former value is in agreement with experiment (−8.0 kcal mol^{-1}), while the lack of experimental data regarding the reaction enthalpy in CM precludes any conclusions to be drawn from the latter result. For comparison, use of a Boltzmann-weighted averaging procedure[31,32] to compute the average activation energy from the five pathways (SI section S2.5) leads to a reduction in the barrier of between 2 and 3 kcal mol^{-1} in both environments. The computed results do not include zero-point energy (ZPE) and enthalpic temperature corrections nor the energetic cost of forming the reactive conformation of the substrate in solution.[1,26] B3LYP frequency calculations by Claeyssens et al. indicate that these ZPE and enthalpic effects reduce the barrier height in a small model of CM by 1.5 and 0.1 kcal mol^{-1}, respectively.[1] Adding these corrections to the computed barriers in Table 2 would slightly improve the agreement between our LS-DFT results and experiment. It should be noted that the reactant conformation of the substrate found in this investigation, which is based on the global minimum in the enzyme, is likely to be one of many local minima present in water. Indeed, the global minimum-energy structure in solution (pseudodiequatorial) has previously been found to occupy a different conformation to the optimal structure in the enzyme (pseudodiaxial).[33] Thus, an associated free-energy difference, estimated to lie between 0.9 and 3.6 kcal mol^{-1}, is likely to contribute to the overall activation and reaction energies in solution.[26,33−35] The remaining discrepancies between computation and experiment are expected to be dominated by inaccuracies in the treatment of electron exchange and correlation; here, we have employed the PBE functional, augmented by damped London energy expressions, to account for dispersion interactions.[36] Currently, these methods represent the state-of-the-art in LS-DFT simulations of enzyme

dx.doi.org/10.1021/jz5018703 | J. Phys. Chem. Lett. 2014, 5, 3614−3619

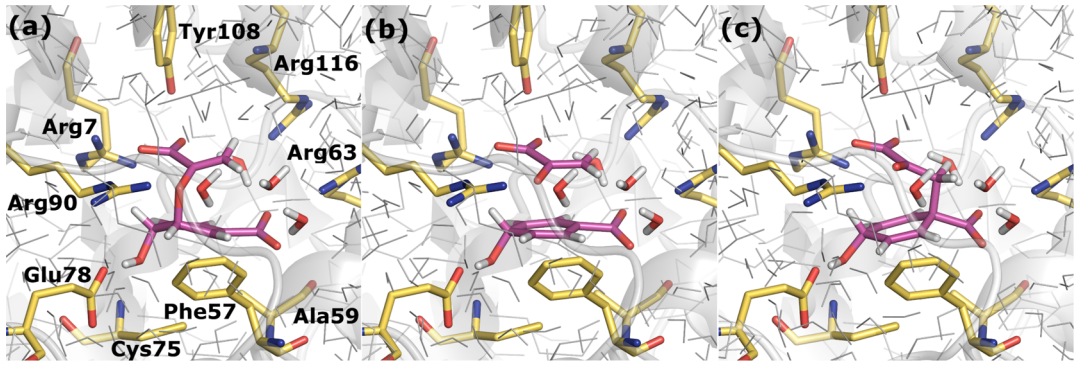

Figure 2. Rearrangement of the substrate (magenta) from chorismate to prephenate within the CM active site (yellow) and surrounding protein (gray). (a) RS, (b) TS, and (c) PS conformations obtained from LS-DFT structural optimization.

Table 2. Energy Difference Comparison[a]

		$\Delta^{\ddagger}E$	ΔE
enzyme	ONETEP	13.6 ± 1.3	−7.8 ± 0.5
	experiment[24]	12.7 ± 0.4	
water	ONETEP	24.1 ± 1.1	−9.4 ± 2.2
	experiment[23]	20.7 ± 0.4	−13.2 ± 0.5

[a]Comparison of averaged activation ($\Delta^{\ddagger}E$) and reaction (ΔE) energies (kcal mol^{-1}) in CM and water with experiment.

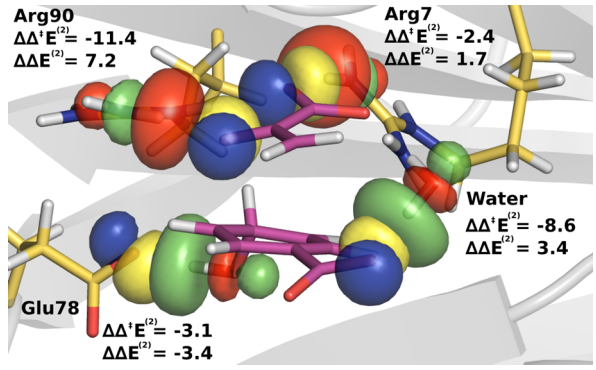

Figure 3. NBOs participating in enzyme−substrate interactions at the TS. Lone pairs (n) are shown as blue/yellow isosurfaces, while antibonding (σ^*) orbitals are in red/green. Electronic delocalization energetic contributions (kcal mol^{-1}) to the stabilization of the TS ($\Delta\Delta^{\ddagger}E^{(2)}$) and the destabilization of the product ($\Delta\Delta E^{(2)}$), relative to the reactant, are also shown.

reactions, though, in the future, it will be possible to use more rigorous treatments of electron exchange and correlation.[37]

While a standard LS-DFT calculation has the potential to improve the accuracy of TS searching in enzymes, it is not immediately clear how to determine the contribution of individual active site residues to TS stabilization. In this respect, it is instructive to transform the nonorthogonal generalized Wannier functions (NGWFs) that are used to describe the electronic structure of the active site of CM into a set of natural bond orbitals (NBOs).[38,39] The resulting NBOs may then be categorized into chemically intuitive Lewis-type bonding and lone pair orbitals, as well as their antibonding counterparts. Electronic delocalization from filled to vacant NBOs causes a variational lowering of the total energy, which can be estimated from second-order perturbation theory ($\Delta E^{(2)}$). This stabilization energy is strongly correlated with the strengths of hydrogen bonds in simple systems,[39,40] and we can therefore use it as a qualitative estimate of the importance of active site residues in the catalytic rate enhancement in CM. Figure 3 shows the four pairs of NBOs that are responsible for the strongest enzyme−substrate charge-transfer interactions. The residues involved are Arg 90 (in agreement with mutagenesis experiments[41] following theoretical predictions[42,43] and experimental proposals[24,44]), Glu 78 (in agreement with other computational studies[45]), Arg 7 (in agreement with previous calculations[46]), and a water molecule. Also shown in Figure 3 are the changes in charge-transfer energetic contributions at the TS ($\Delta\Delta^{\ddagger}E^{(2)}$) and the PS ($\Delta\Delta E^{(2)}$) relative to the RS. In all cases, electronic delocalization acts to stabilize the TS and (apart from Glu78) destabilize the PS. It can be useful to compare the interactions in the enzyme with those in solution when discussing the contributions to catalysis.[47] In contrast with our findings in CM, in solution, it is found that interactions with water may either stabilize or destabilize the substrate at the TS, relative to the RS, because contributions to $\Delta\Delta^{\ddagger}E^{(2)}$ from individual water molecules vary in the range of +4.2 to −4.6 kcal mol^{-1}. The observation of strong stabilization interactions in the presence of the enzyme suggests that the structure has evolved to provide more significant orbital overlap between charged residues and the substrate at the TS, thus lowering the activation energy barrier. This picture is supported by previous calculations that have demonstrated that the catalytic effect of the enzyme is dominated by electrostatic TS stabilization.[1,25,48]

This Letter demonstrates the feasibility of modeling reactions, including optimizing TS structures, in enzymes by quantum mechanical treatment of the substrate and a large portion of its environment. The activation and reaction energies are in good agreement with experiment and, more importantly, are shown to be converged with respect to system size and virtually independent of computational parameters. Although the five reaction pathways considered in this relatively simple reaction have similar energies of activation and reaction, for more flexible proteins, it is likely that a larger number of pathways would need to be considered and that alternative averaging schemes, such as Boltzmann-averaging,[31,32] would become more important.[49] Calculations such as those presented in this Letter will be an important test of QM/MM modeling, they will help identify cases in which MM treatments of the protein environment may fail, and they will allow analysis of large-scale electronic effects. In CM, the excellent structural agreement between DFT-based QM/MM and linear-scaling QM results is very encouraging, and the

dx.doi.org/10.1021/jz5018703 | J. Phys. Chem. Lett. 2014, 5, 3614−3619

methods concur in showing that stabilization of the TS in the enzyme is at the root of catalysis.

COMPUTATIONAL METHOD

In this Letter, computational TS searching in the CM enzyme has been performed using the ONETEP DFT code.[21] By making use of a minimal set of strictly localized NGWFs which are optimized in situ, ONETEP combines a computational cost that scales linearly with the number of atoms in the system[50] with the accuracy of more conventional plane wave DFT codes. The NGWFs are further expanded in a basis set of periodic sinc (psinc) functions,[51] which may be systematically improved through varying a single kinetic energy cutoff parameter. All calculations were performed using the PBE generalized gradient approximation[27] and norm-conserving pseudopotentials. van der Waals interactions were approximated by augmenting the DFT energy with damped London potentials.[36] Interactions between molecules and their periodic images were eliminated through the use of the spherical cutoff Coulomb approach.[52]

Ionic forces in ONETEP[28] are calculated by an application of the Hellman−Feynman theorem,[53,54] including Pulay corrections,[55] and, during geometry optimization, are minimized in a quasi-Newton scheme[56] using the Broyden−Fletcher−Goldfarb−Shanno (BFGS) algorithm.[57] Full details of the implementation and comparison with plane wave pseudopotential approaches can be found in ref 28. Geometry optimization requires a number of evaluations of the potential energy surface, and this number is expected to increase with the number of atoms in the system.[58] Initial steps toward reducing this computational burden within a large-scale simulation framework have been taken by other authors.[10,59−61] It has been argued that, in practical terms, it is sufficient to only relax a smaller subregion of a larger system, introducing a level of tractability into the optimization, especially when studying the effect of a localized change of conformation on an otherwise relaxed system.[28] It has also been shown there are no large-scale conformational changes during enzymatic activity in CM;[62−64] therefore, the enzyme lends itself naturally to this type of optimization procedure. However, it is also important to show that the calculated properties of interest are converged with respect to the size of the optimization region used (see Tables 1 and S1, SI).

TS searching calculations were performed according to a modified linear synchronous transit (LST) and quadratic synchronous transit (QST) pathway approach[65] in combination with the conjugate gradient (CG) optimization implemented in ONETEP.[29] In the LST approach, a set of structures connecting the reactant and product is obtained by linearly interpolating internuclear distances between the two BFGS-optimized end points. The tangent to the trajectory at the energy maximum of this path defines the direction of negative curvature. CG optimizations are then performed at the energy maximum, and the resulting structure is used as a TS guess in a new QST path connecting the reactant and product. CG and QST cycles are subsequently repeated until convergence has been achieved, which in principle should result in the true TS connecting the minima, which is defined as the configuration yielding a single negative Hessian eigenvalue.[66]

ASSOCIATED CONTENT

Supporting Information

The QM/MM and full-QM system setup, ONETEP parameters (including electrostatic embedding, implicit solvation, structural optimization details, LST/QST searching, and natural bond orbital analysis), eigenvector-following calculations, and the Boltzmann-weighted averaging of the energy barriers. This material is available free of charge via the Internet at http://pubs.acs.org.

AUTHOR INFORMATION

Corresponding Author

*E-mail: gl319@cam.ac.uk.

Notes

The authors declare no competing financial interest.

ACKNOWLEDGMENTS

The authors are grateful to Louis Lee (University of Cambridge) for helpful discussions and Karl Wilkinson (University of Southampton) for modifications to the ONETEP code. Computational resources were provided by the Cambridge HPC Service, funded by EPSRC Grants EP/F032773/1 and EP/J017639/1, by the IRIDIS3 supercomputer of the University of Southampton, and by the HECToR national supercomputer, funded by EPSRC Grant EP/F038038/1 (UKCP consortium). The authors are grateful for funding provided by the EPSRC (G.L., R.L., K.E.R., D.J.W., and A.J.M.), specifically R.L. and A.J.M. for support under the CCP-BioSim project (Grant EP/J010588/1; www.ccpbiosim.ac.uk) and A.J.M. as an EPSRC Leadership Fellow (Grant EP/G007705/01). The authors also acknowledge a Marie Curie International Outgoing Fellowship within the 7th European Community Framework Programme (D.J.C.), the Royal Society (C.-K.S.), and the ERC (D.J.W.).

REFERENCES

(1) Claeyssens, F.; Harvey, J. N.; Manby, F. R.; Mata, R. A.; Mulholland, A. J.; Ranaghan, K. E.; Schütz, M.; Thiel, S.; Thiel, W.; Werner, H. J. High-Accuracy Computation of Reaction Barriers in Enzymes. *Angew. Chem., Int. Ed.* **2006**, *45*, 6856−6859.

(2) Solt, I.; Kulhànek, P.; Simon, I.; Winfield, S.; Payne, M. C.; Csànyi, G.; Fuxreiter, M. Evaluating Boundary Dependent Force Errors in QM/MM Simulations. *J. Phys. Chem. B* **2009**, *113*, 5728−5735.

(3) Neugebauer, J. Subsystem-Based Theoretical Spectroscopy of Biomolecules and Biomolecular Assemblies. *Chem. Phys. Chem.* **2009**, *10*, 3148−3173.

(4) Lee, L. P.; Cole, D. J.; Skylaris, C.-K.; Jorgensen, W. L.; Payne, M. C. Polarized Protein-Specific Charges from Atoms-in-Molecule Electron Density Partitioning. *J. Chem. Theory Comput.* **2013**, *9*, 2981−2991.

(5) Lever, G.; Cole, D. J.; Hine, N. D. M.; Haynes, P. D.; Payne, M. C. Electrostatic Considerations Affecting the Calculated HOMO−LUMO Gap in Protein Molecules. *J. Phys.: Condens. Matter* **2013**, *25*, 152101.

(6) Khaliullin, R. Z.; VandeVondele, J.; Hutter, J. Efficient Linear-Scaling Density Functional Theory for Molecular Systems. *J. Chem. Theory Comput.* **2013**, *9*, 4421−4427.

(7) Hine, N. D. M.; Haynes, P. D.; Mostofi, A. A.; Skylaris, C.-K.; Payne, M. C. Linear-Scaling Density-Functional Theory with Tens of Thousands of Atoms: Expanding the Scope and Scale of Calculations with ONETEP. *Comput. Phys. Commun.* **2009**, *180*, 1041−1053.

(8) Iwata, J. I.; Takahashi, D.; Oshiyama, A.; Boku, T.; Shiraishi, K.; Okada, S.; Yabana, K. A Massively-Parallel Electronic-Structure Calculations Based on Real-Space Density Functional Theory. *J. Comput. Phys.* **2010**, *229*, 2339−2363.

(9) Cole, D. J.; Chin, A. W.; Hine, N. D. M.; Haynes, P. D.; Payne, M. C. Toward Ab Initio Optical Spectroscopy of the Fenna−Matthews−Olson Complex. *J. Phys. Chem. Lett.* **2013**, *4*, 4206−4212.

(10) Cole, D. J.; O'Regan, D. D.; Payne, M. C. Ligand Discrimination in Myoglobin from Linear-Scaling DFT+*U*. *J. Phys. Chem. Lett.* **2012**, *3*, 1448−1452.
(11) Weber, C.; Cole, D. J.; O'Regan, D. D.; Payne, M. C. Renormalization of Myoglobin−Ligand Binding Energetics by Quantum Many-Body Effects. *Proc. Natl. Acad. Sci. U.S.A.* **2014**, *111*, 5790−5795.
(12) Tkatchenko, A.; Rossi, M.; Blum, V.; Ireta, J.; Scheffler, M. Unraveling the Stability of Polypeptide Helices: Critical Role of van der Waals Interactions. *Phys. Rev. Lett.* **2011**, *106*, 118102.
(13) Kulik, H. J.; Luehr, N.; Ufimtsev, I. S.; Martínez, T. J. Ab Initio Quantum Chemistry for Protein Structures. *J. Phys. Chem. B* **2012**, *116*, 12501−12509.
(14) de Pablo, P. J.; Moreno-Herrero, F.; Colchero, J.; Herrero, J. G.; Herrero, P.; Baró, A. M.; Ordejón, P.; Soler, J. M.; Artacho, E. Absence of dc-Conductivity in λ-DNA. *Phys. Rev. Lett.* **2000**, *85*, 4992−4995.
(15) T, T. O.; Miyazaki, T.; Ohno, T.; Bowler, D. R.; Gillan, M. J. Accuracy of Order-N Density-Functional Theory Calculations on DNA Systems Using CONQUEST. *J. Phys.: Condens. Matter* **2008**, *20*, 294201.
(16) Bondesson, L.; Rudberg, E.; Luo, Y.; Sałek, P. A Linear Scaling Study of Solvent−Solute Interaction Energy of Drug Molecules in Aqua Solution. *J. Phys. Chem. B* **2007**, *111*, 10320−10328.
(17) Ozaki, T. Efficient Low-Order Scaling Method for Large-Scale Electronic Structure Calculations with Localized Basis Functions. *Phys. Rev. B* **2010**, *82*, 075131.
(18) Todorović, M.; Bowler, D. R.; Gillan, M. J.; Miyazaki, T. Density-Functional Theory Study of Gramicidin A Ion Channel Geometry and Electronic Properties. *J. R. Soc., Interface* **2013**, *10*, 20130547.
(19) Goedecker, S. Linear Scaling Electronic Structure Methods. *Rev. Mod. Phys.* **1999**, *71*, 1085−1123.
(20) Bowler, D. R.; Miyazaki, T. *O*(N) Methods in Electronic Structure Calculations. *Rep. Prog. Phys.* **2012**, *75*, 036503.
(21) Skylaris, C.-K.; Haynes, P. D.; Mostofi, A. A.; Payne, M. C. Introducing ONETEP: Linear-Scaling Density Functional Simulations on Parallel Computers. *J. Chem. Phys.* **2005**, *122*, 084119.
(22) Kast, P.; Tewari, Y. B.; Wiest, O.; Hilvert, D.; Houk, K. N.; Goldberg, R. N. Thermodynamics of the Conversion of Chorismate to Prephenate: Experimental Results and Theoretical Predictions. *J. Phys. Chem. B* **1997**, *101*, 10976−10982.
(23) Andrews, P. R.; Smith, G. D.; Young, I. G. Transition-State Stabilization and Enzymic Catalysis. Kinetic and Molecular Orbital Studies of the Rearrangement of Chorismate to Prephenate. *Biochemistry* **1973**, *12*, 3492−3498.
(24) Kast, P.; Asif-Ullah, M.; Hilvert, D. Is Chorismate Mutase a Prototypic Entropy Trap? − Activation Parameters for the Bacillus Subtilis Enzyme. *Tetrahedron Lett.* **1996**, *37*, 2691−2694.
(25) Crespo, A.; Scherlis, D. A.; Marti, M. A.; Ordejon, P.; Roitberg, A. E.; Estrin, D. A. A DFT-Based QM−MM Approach Designed for the Treatment of Large Molecular Systems: Application to Chorismate Mutase. *J. Phys. Chem. B* **2003**, *107*, 13728−13736.
(26) Claeyssens, F.; Ranaghan, K. E.; Lawan, N.; Macrae, S. J.; Manby, F. R.; Harvey, J. N.; Mulholland, A. J. Analysis of Chorismate Mutase Catalysis by QM/MM Modelling of Enzyme-Catalysed and Uncatalysed Reactions. *Org. Biomol. Chem.* **2011**, *9*, 1578−1590.
(27) Perdew, J. P.; Burke, K.; Enzerhof, M. Generalized Gradient Approximation Made Simple. *Phys. Rev. Lett.* **1996**, *77*, 3865−3868.
(28) Hine, N. D. M.; Robinson, M.; Haynes, P. D.; Skylaris, C.-K.; Payne, M. C.; Mostofi, A. A. Accurate Ionic Forces and Geometry Optimization in Linear-Scaling Density-Functional Theory with Local Orbitals. *Phys. Rev. B* **2011**, *83*, 195102.
(29) Govind, N.; Petersen, M.; Fitzgerald, G.; King-Smith, D.; Andzelm, J. A Generalized Synchronous Transit Method for Transition State Location. *Comput. Mater. Sci.* **2003**, *28*, 250−258.
(30) Munro, L. J.; Wales, D. J. Defect Migration in Crystalline Silicon. *Phys. Rev. B* **1999**, *59*, 3969−3980.
(31) Lonsdale, R.; Harvey, J. N.; Mulholland, A. J. Compound I Reactivity Defines Alkene Oxidation Selectivity in Cytochrome P450cam. *J. Phys. Chem. B* **2010**, *114*, 1156−1162.
(32) Lonsdale, R.; Houghton, K. T.; Žurek, J.; Bathelt, C. M.; Foloppe, N.; de Groot, M. J.; Harvey, J. N.; Mulholland, A. J. Quantum Mechanics/Molecular Mechanics Modeling of Regioselectivity of Drug Metabolism in Cytochrome P450 2C9. *J. Am. Chem. Soc.* **2013**, *135*, 8001−8015.
(33) Copley, S. D.; Knowles, J. R. The Conformational Equilibrium of Chorismate in Solution: Implications for the Mechanism of the Non-Enzymic and the Enzyme-Catalyzed Rearrangement of Chorismate to Prephenate. *J. Am. Chem. Soc.* **1987**, *109*, 5008−5013.
(34) Martí, S.; Andrés, J.; Moliner, V.; Silla, E.; nón, I. T.; Bertrán, J. Conformational Equilibrium of Chorismate. A QM/MM theoretical Study Combining Statistical Simulations and Geometry Optimisations in Gas Phase and in Aqueous Solution. *J. Mol. Struct.: THEOCHEM* **2003**, *632*, 197−206.
(35) Carlson, H. A.; Jorgensen, W. L. Monte Carlo Investigations of Solvent Effects on the Chorismate to Prephenate Rearrangement. *J. Am. Chem. Soc.* **1996**, *118*, 8475−8484.
(36) Hill, Q.; Skylaris, C.-K. Including Dispersion Interactions in the ONETEP Program for Linear-Scaling Density Functional Theory Calculations. *Proc. R. Soc. London, Ser. A* **2009**, *465*, 669−683.
(37) Dziedzic, J.; Hill, Q.; Skylaris, C.-K. Linear-Scaling Calculation of Hartree−Fock Exchange Energy with Non-Orthogonal Generalised Wannier Functions. *J. Chem. Phys.* **2013**, *139*, 214103.
(38) Glendening, E. D.; Badenhoop, J. K.; Reed, A. E.; Carpenter, J. E.; Bohmann, J. A.; Morales, C. M.; Weinhold, F. *NBO 5*; Theoretical Chemistry Institute, University of Wisconsin: Madison, WI, 2001.
(39) Lee, L. P.; Cole, D. J.; Payne, M. C.; Skylaris, C.-K. Natural Bond Orbital Analysis in the ONETEP Code: Applications to Large Protein Systems. *J. Comput. Chem.* **2013**, *34*, 429−444.
(40) Mohajeri, A.; Nobandegani, F. F. Detection and Evaluation of Hydrogen Bond Strength in Nucleic Acid Base Pairs. *J. Phys. Chem. A* **2008**, *112*, 281−295.
(41) Cload, S. T.; Liu, D. R.; Pastor, R. M.; Schultz, P. G. Mutagenesis Study of Active Site Residues in Chorismate Mutase from Bacillus Subtilis. *J. Am. Chem. Soc.* **1996**, *118*, 1787−1788.
(42) Lyne, P. D.; Mulholland, A. J.; Richards, W. G. Insights Into Chorismate Mutase Catalysis from a Combined QM/MM Simulation of the Enzyme Reaction. *J. Am. Chem. Soc.* **1995**, *17*, 11345−11350.
(43) Guimaraēs, C. R. W.; Udier-Blagović, M.; Tubert-Brohman, I.; Jorgensen, W. L. Contributions of Conformational Compression and Preferential Transition State Stabilization to the Rate Enhancement by Chorismate Mutase. *J. Am. Chem. Soc.* **2003**, *125*, 6892−6899.
(44) Gorisch, H. On the Mechanism of the Chorismate Mutase Reaction. *Biochemistry* **1978**, *3700−3705*, 17.
(45) Worthington, S. E.; Roitberg, A. E.; Krauss, M. An MD/QM Study of the Chorismate Mutase-Catalyzed Claisen Rearrangement Reaction. *J. Phys. Chem. B* **2001**, *105*, 7087−7095.
(46) Lee, Y. S.; Worthington, S. E.; Krauss, M.; Brooks, B. R. Reaction Mechanism of Chorismate Mutase Studied by the Combined Potentials of Quantum Mechanics and Molecular Mechanics. *J. Phys. Chem. B* **2002**, *106*, 12059−12065.
(47) Yang, Y.; Cui, Q. The Hydrolysis Activity of Adenosine Triphosphate in Myosin: A Theoretical Analysis of Anomeric Effects and the Nature of the Transition State. *J. Phys. Chem. A* **2009**, *113*, 12439−12446.
(48) Szefczyk, B.; Mulholland, A. J.; Ranaghan, K. E.; Sokalski, W. A. Differential Transition-State Stabilization in Enzyme Catalysis: Quantum Chemical Analysis of Interactions in the Chorismate Mutase Reaction and Prediction of the Optimal Catalytic Field. *J. Am. Chem. Soc.* **2004**, *126*, 16148−16159.
(49) Lonsdale, R.; Harvey, J. N.; Mulholland, A. J. A Practical Guide to Modelling Enzyme-Catalysed Reactions. *Chem. Soc. Rev.* **2012**, *41*, 3025−3038.
(50) Skylaris, C.-K.; Haynes, P. D.; Mostofi, A. A.; Payne, M. C. Implementation of Linear-Scaling Plane Wave Density Functional

Theory on Parallel Computers. *Phys. Status Solidi B* **2006**, *243*, 973−988.
(51) Mostofi, A. A.; Haynes, P. D.; Skylaris, C.-K.; Payne, M. C. Preconditioned Iterative Minimisation for Linear-Scaling Electronic Structure Calculations. *J. Chem. Phys.* **2003**, *119*, 8842−8848.
(52) Hine, N.; Dziedzic, J.; Haynes, P. D.; Skylaris, C.-K. Electrostatic Interactions in Finite Systems treated with Periodic Boundary Conditions: Application to Linear-Scaling Density Functional Theory. *J. Chem. Phys.* **2011**, *135*, 204103.
(53) Hellman, H. *Einführung in die Quanten Theorie*; Deuticke: Leipzig, Germany, 1937; p 285.
(54) Feynman, R. P. Forces in Molecules. *Phys. Rev.* **1939**, *56*, 340−343.
(55) Ruiz-Serrano, A.; Hine, N. D. M.; Skylaris, C.-K. Pulay Forces from Localized Orbitals Optimized In Situ Using a Psinc Basis Set. *J. Chem. Phys.* **2012**, *136*, 234101.
(56) Pfrommer, B. G.; Côté, M.; Louie, S. G.; Cohen, M. L. Relaxation of Crystals with the Quasi-Newton Method. *J. Comput. Phys.* **1997**, *131*, 233−240.
(57) Nocedal, J.; Wright, S. J. *Numerical Optimization*; Springer-Verlag: New York, 2006.
(58) Goedecker, S.; Lançon, F.; Deutsch, T. Linear Scaling Relaxation of the Atomic Positions in Nanostructures. *Phys. Rev. B* **2001**, *64*, 161102(R).
(59) Fernández-Serra, M. V.; Artacho, E.; Soler, J. M. Model Hessian for Accelerating First-Principles Structure Optimizations. *Phys. Rev. B* **2003**, *67*, 100101(R).
(60) Nemeth, K.; Challacombe, M. The Quasi-Independent Curvilinear Coordinate Approximation for Geometry Optimization. *J. Chem. Phys.* **2004**, *121*, 2877−2885.
(61) Nemeth, K.; Challacombe, M. Geometry Optimization of Crystals by the Quasi-Independent Curvilinear Coordinate Approximation. *J. Chem. Phys.* **2005**, *123*, 194112.
(62) Chook, Y. M.; Ke, H.; Lipscomb, W. N. Crystal Structures of the Monofunctional Chorismate Mutase from Bacillus subtilis and Its Complex with a Transition State Analog. *Proc. Natl. Acad. Sci. U.S.A.* **1993**, *90*, 8600−8603.
(63) Chook, Y. M.; Gray, J. V.; Ke, H.; Lipscomb, W. N. Conformational and Solvation Aspects of the Chorismate−Prephenate Rearrangement Studied by Ab Initio Electronic Structure and Simulation Methods. *J. Mol. Biol.* **1994**, *240*, 476−500.
(64) Eletsky, A.; Kienhöfer, A.; Hilvert, D.; Pervushin, K. Investigation of Ligand Binding and Protein Dynamics in Bacillus Subtilis Chorismate Mutase by Transverse Relaxation Optimized Spectroscopy-Nuclear Magnetic Resonance. *Biochemistry* **2005**, *44*, 6788−6799.
(65) Halgren, T. A.; Lipscomb, W. N. The Synchronous-Transit Method for Determining Reaction Pathways and Locating Molecular Transition States. *Chem. Phys. Lett.* **1977**, *49*, 225−232.
(66) Murrell, J. N.; Laidler, K. J. Symmetries of Activated Complexes. *Trans. Faraday Soc.* **1968**, *67*, 371−377.